AIChE WILEY InterScience DISCOVER SOMETHING GREAT

Visualization of the Flow of a Fiber Suspension Through a Sudden Expansion Using PET

S. J. Heath and J. A. Olson
Dept. of Mechanical Engineering, University of British Columbia, 2054-6250 Applied Science Lane, Vancouver, BC, V6T 1Z4, Canada

K. R. Buckley, S. Lapi, and T. J. Ruth
TRIUMF, 4004 Wesbrook Mall, Vancouver, BC, V6T 2A3, Canada

D. M. Martinez
Dept. of Chemical and Biological Engineering, University of British Columbia, 2360 Main Mall Vancouver BC, V6T 1Z3, Canada

DOI 10.1002/aic.11084
Published online January 4, 2007 in Wiley InterScience (www.interscience.wiley.com).

The motion of ^{18}F radioactively labeled papermaking fibers flowing through an axisymmetric 1:5 sudden expansion has been studied using positron emission tomography (PET). Various length fractions of a mechanical pulp were radioactively labeled and then introduced into a nonradioactive aqueous 0.4 wt. % (consistency) wood pulp suspension. Fully three-dimensional (3-D) images were reconstructed both upstream and downstream of the expansion plane for cases in which the upstream velocity U was set from 0.5 to 0.9 m/s (an approximate Reynolds number range of 7,000 to 13,000). Two distinct flow regimes were clearly identified. With U ~ 0.5 m/s we find that the fiber suspension was not fluidized, and the tracer fibers passed through the expansion as a plug. No mixing was observed between the confined central jet and the static outer region. At larger velocities, we observed that the papermaking suspension was fully fluidized. Our results in this regime indicate that albeit fluidized, concentration inhomogeneities were evident. We find that a particle depletion zone was evident between the central jet, and the recirculating zone resulting from the inlet concentration profile formed in the upstream tube. Particle accumulation was observed in the vortices. No significant differences were observed between the different length tracer fibers.
© 2007 American Institute of Chemical Engineers *AIChE J,* 53: 327–334, 2007

Introduction

The focus of the present work is an experimental study of the concentration distribution of a semidilute fiber suspension-undergoing steady flow in an abrupt 1:5 sudden expansion. Although the flow of multiphase fluids through sudden expansions is found in many industrial and natural settings, there are still many unanswered questions regarding the mechanism of particle dispersion (fluidization) or clumping (flocculation). The motivation for this work stems from an interest in the papermaking process. Under normal processing conditions, papermaking suspensions mechanically entangle to form a network, which possesses a measurable yield stress (Thalen and Wahren, 1964a,b; Duffy and Titchener, 1975). During processing the suspension is fluidized into individual flocs or fibers, with weakly correlated velocities, by turbu-

Correspondence concerning this article should be addressed to D. M. Martinez at martinez@chml.ubc.ca.

© 2007 American Institute of Chemical Engineers

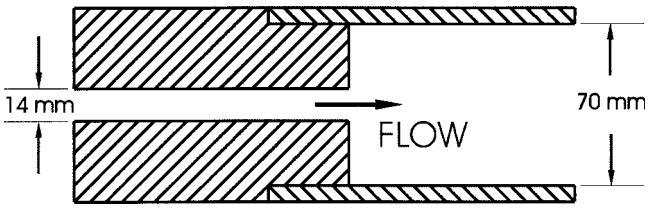

Figure 1. Sudden expansion.

lence created locally by an abrupt expansion. This aids in evenly dispersing the suspension. In a papermachine, sudden expansions are found in the crossflow distributor, the turbulence generator, and the headbox nozzle. Suspensions, which are evenly dispersed, reduce the cloudiness or graininess of the sheet and aid in the elimination of grammage (areal density) variations, a property that is important for all paper grades. While the objectives of the papermaking process are clear, and the equipment on the paper machine well known, the exact mechanism by which fluidization and material redistribution occurs remains obscure. Our objective is to provide insight into this phenomenon by visualizing the flow of the papermaking suspension through a sudden expansion using positron emission tomography (PET).

Understanding the motion of an aqueous fiber suspension flowing through a sudden expansion is difficult. Insight into this phenomena can be gained by first examining the simpler case of the flow of single-phase fluid. For Newtonian fluids, Macagno and Hung (1967) indicate that over all Reynolds numbers, a vortex exists immediately downstream of the expansion. There is general agreement that at low *Re* the size of the vortex increases linearly with Reynolds number and then decreases with $Re > 635$ (Latornell and Pollard, 1986). In contrast with this, non-Newtonian fluids exhibit vortex lengths that differ significantly from Newtonian fluids. With yield stress fluids, the recirculation lengths were found to be smaller when compared to Newtonian fluids at a comparable Reynolds number (Hammad et al. 1999; Jossic et al., 2002).

The case of expansion flows with particle suspensions remains largely unexplored. This class of flow is strikingly different than single-phase flows as particle concentration inhomogenieties are generated through particle collisions, shear induced particle migration (Leighton and Acrivos, 1987; Phillips et al., 1992), density differences between the particles and the carrier fluid, inertia, and, in the case of papermaking fibers, flocculation created through frictional forces between the particles (Kerekes et al., 1985). To help illustrate this complexity, there is evidence that with suspensions of neutrally buoyant monodisperse spheres, particle accumulation or depletion is evident in the vortex, depending on the ratio of the upstream tube to particle diameters (Altobelli et al., 1997a; Altobelli et al., 1997b; Karino and Goldsmith, 1977). In a recent study, Moraczewski et al. (2005) observe that a low-concentration region exists, which divides the central jet and the recirculation region. They attribute this to inhomogeneities in the inlet concentration that were convected downstream. The concentration profiles in this case were measured using nuclear magnetic-resonance imaging (NMR) after the flow had been stopped.

With regards to papermaking suspensions, there is evidence of seemingly two different behavious. Arola et al. (1998), for example, imaged the axial velocity profile of a 0.5% (wt) wood pulp suspension flowing through a 1:1.7 sudden expansion using NMR. These authors report that the pulp suspension exhibited behavior similar to that of a confined jet. In recent work, Salmela and Kataja (2005) used an optical technique to measure the floc size and fiber flow field of a semidilute suspension after the expansion. They report that the recirculation eddy downstream of the expansion plane was found only to exist when the step height exceeds the mean fiber length. When existing, the suspension was fluidized and behaved as a Newtonian fluid.

Our work is focused on complimenting these previous studies by measuring the steady-state concentration profiles of papermaking fibers as they pass through a sudden expansion. Here, the behavior of Fluorine-18 (^{18}F) labeled papermaking fibers flowing in the midst of nonradioactive fibers are studied using PET. We measure the radioactivity distribution, three-dimensionally, near the expansion plane, and then far downstream of the expansion plane. The experimental conditions were such that the bulk concentration of the suspension was fixed, while we varied the volumetric flow rate, and size of the ^{18}F labeled fibers. The key advantage of this measurement technique is that the concentration profile can be determined for each particle fraction directly without stopping the flow. In addition, we measure the axial velocity of the suspension far downstream of the expansion plane using pulsed ultrasound Doppler anemometry (UDV).

Materials and Methods

The closed-loop system used for these experiments consists of a 120 *L* tank, a centrifugal pump, a bypass loop, two magnetic flow meters, two pressure transducers, a test section and valves for control. The test section is made of clear polycarbonate pipe 70 mm in diameter and 1.1 m in length. The inlet pipe is 14 mm in diameter forming a 1:5 axisymmetric sudden expansion. Figure 1 shows a cross-sectional view of

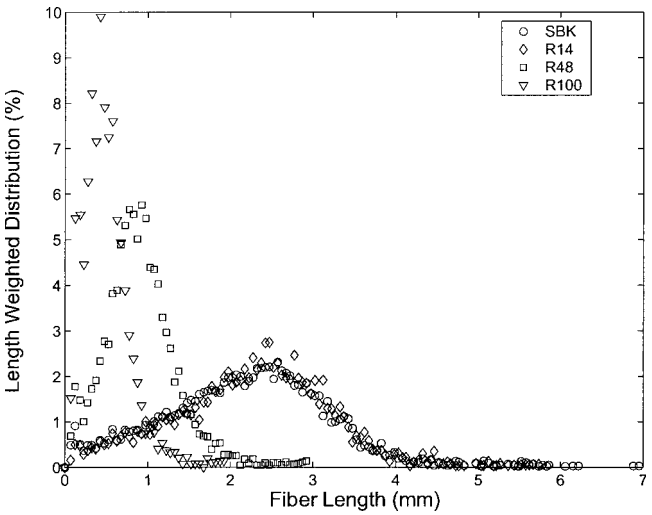

Figure 2. Fiber-length distributions of the SBK pulp and the three tracer fibers used (labeled R14, R48 and R100).

The notation for the fiber fractions is retained from the Bauer Mcnett device used to separate the fiber suspension.

Table 1. A Summary of the Scans Conducted

Scan	Tracer (fraction)	Upstream Vel. (*m/s*)	Activity (*M Bq*)	Image Dur. Step (*s*)	Image Dur. Downstream (s)	Phenom. Behavior
1	R48	0.5	585	3599	2736	plug
2	R48	0.7	480	2212	2922	fluidized
3	R48	0.8	1125	2708	2289	fluidized
4	R14	0.5	1015	2573	2197	partially-fluidized
5	R14	0.9	1045	1220	1134	fluidized
6	R100	0.9	475	2772	3072	fluidized

the abrupt expansion. Flow reaches and leaves the test section through 4.5 m of reinforced hose which ensures fully developed flow at the expansion step for all cases studied. Both ends of the test section are terminated with a pair of full-bore ball valves, and a full-bore quick-disconnect coupling to facilitate placement and removal of the test section into the gantry of the tomograph. The test section is mounted to 760 mm linear stages on either side of the tomograph so that the test section can be moved along its axis. To shield the detector blocks from radiation originating outside the tomograph 19 mm thick lead shielding is positioned concentrically with the test section, butted up against the camera. This thickness of lead stops 95% of incoming 511 *keV* gamma photons.

The experiments were conducted by first radioactively labeling a selected Bauer-McNett fraction of themomechanical pulp (TMP) fibers with ^{18}F, and introducing this into a nonradioactive pulp suspension. The fiber length of each fraction of fibers, and the whole suspension, as determined through use of an optical fiber length analyzer are provided in Figure 2. As shown, the names of the fiber fractions are defined using the screen sizes by which they were retained in the Bauer-McNett device. This is the traditional method of defining fiber fractions in the pulp and paper literature. The fibers were labeled by suspending them in a solution of acetic acid while $^{18}F - F_2$ was bubbled through the suspension at 10 ml/min with constant stirring. After the addition of the fluorine the fibers were filtered and washed with distilled water. At this point the fibers were labeled with ^{18}F with a 10% yield, based upon the total radioactivity introduced. ^{18}F has been chosen here in preference to other positron emitting tracers such as ^{15}O, ^{11}C, or ^{13}N because of its reasonably long half-life of 110 min, and its reactivity with TMP pulp fibers.

Positron emission tomography is an imaging technique widely used in diagnostic medicine, but has recently been applied to engineering studies. Each emitted positron travels a short distance before annihilating with an electron. This annihilation produces two high-energy (511 keV) photons propagating in opposite directions. If two photons are detected in a short timing window ($\sim$ 10 *ns*) an event is recorded along a line close to which the radioactive decay must have occurred. By detecting many of these events, the

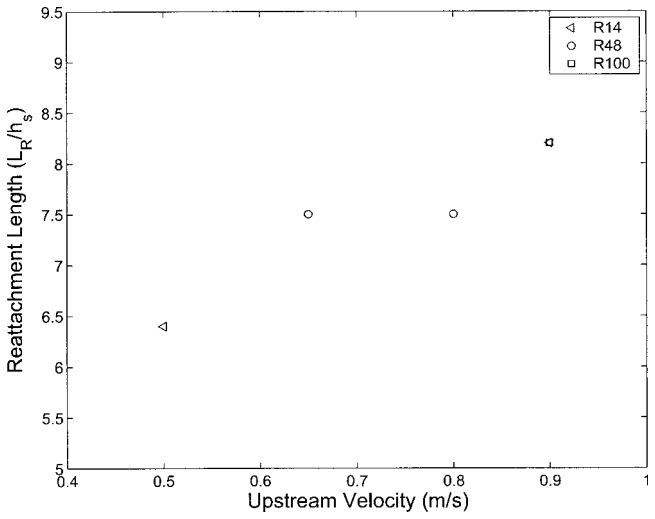

Figure 3. Estimates of the size of the recirculation zone for the cases in which the suspension was fluidized after the expansion.

h_s is the step height.

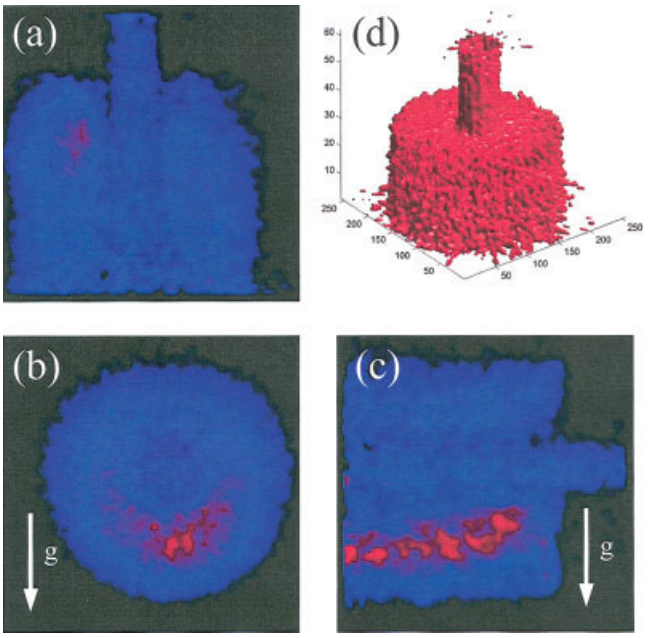

Figure 4. Four views of the activity profile for the case in which the tracer fibers were well-mixed or fluidized after the expansion.

The image was acquired using the R48 tracer fibers with the upstream velocity set at 0.7 *m/s* (see Table 1). Image (a) represents the top view, (b) is a cross-sectional view at $x/R_o = 0.57$, (c) is a side-view, and (d) is a 3-D reconstruction of the activity distribution. No color map is included in (a) through (c), but the blue represents a lower concentration than the red. [Color figure can be viewed in the online issue, which is available at www.interscience.wiley.com.]

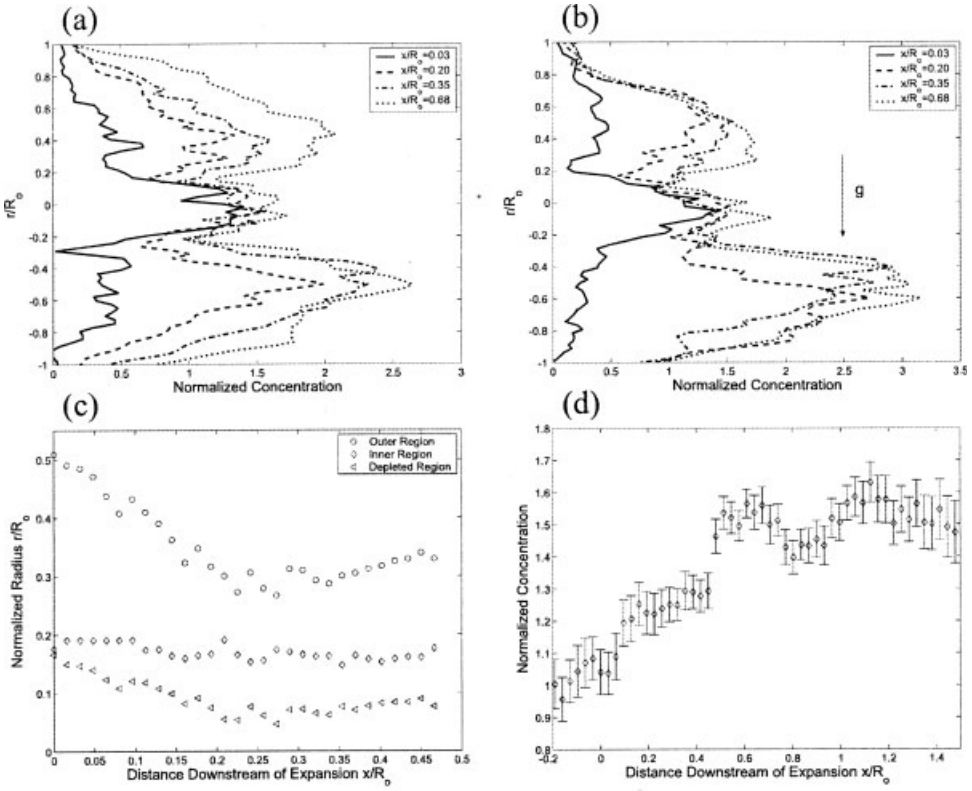

Figure 5. Four views of the activity profile for the case in which the tracer fibers were well-mixed or fluidized after the expansion.

The image was acquired using the R48 tracer fibers with the upstream velocity set at 0.7 *m/s* (see Table 1). Image (a) represents the concentration profile in the radial direction at four different axial positions. This data was acquired from Figure 4a. Image (b) represents the concentration profile in the radial direction at four different axial positions. This data was acquired from Figure 4c. Image (c) is an estimate of the growth of the depletion zone. Estimates are given of the inner and outer radii of the depletion zone and their difference. Image (d) is an estimate of the average concentration of the jet as a function of axial position.

distribution of activity can be determined. The tomograph used in this study is the Concorde Microsystems microPET R4. The microPET Rodent 4-ring system (R4) has a 7.8 cm axial extent, a 10 cm transaxial field of view (FOV), and a 12 cm gantry aperture. The system is composed of 96 detector modules, each with an 8 × 8 array of 2.1 × 2.1 × 10 mm lutetium oxyorthosilicate (LSO) crystals, arranged in 32 crystal rings 14.8 cm in diameter. Each of the detector crystals are coupled to a Hamamatsu R5900-C8 position sensitive photomultiplier tube (PS-PMT) via a 10 cm long optical fiber bundle. The detectors have a timing resolution of 3.2 *ns*, an average energy resolution of 18.45%, and an average intrinsic-spatial resolution of 1.75 mm. The system operates in 3-D mode without interplane septa, acquiring data in list mode. Using the 2-D filtered back projection reconstruction algorithm, the resolution in the center of the field of view (FOV) is 2.03 mm FWHM in the tangential direction (horizontal direction of the FOV), and 2.07 mm FWHM in the radial direction (vertical direction of the FOV). The tangential resolution slowly increases to 3.38 mm FWHM (full width at half maximum) at the edge of the FOV. The radial resolution increases to 3.00 mm FWHM at 25 mm radial offset, and then deteriorates linearly to 3.68 mm FWHM at the edge of the FOV. All images in this study were reconstructed using the 2-D filtered back projection algorithm (Mok et al., 2003). Further information on the PET technique and, in particular, the camera used in this study may be found in Knoess et al. (2003); or Sossi et al. (2005); or the references contained therein.

Table 1 provides the fraction labeled, the upstream bulk flow rate, duration of scans, and activity added for each image obtained in this study. For each case an image was captured at the step and another 70 cm downstream of the expansion. Each scan begins with the production of the labeled fractions. Meanwhile the flow-loop is set up around the microPET scanner. After the test section has been placed in the gantry of the scanner and plumbed in, it is positioned in the cameras field of view with the aid of a laser line. Prior to the emission scan, a transmission scan is performed to characterize the effects of attenuation of the photons due to the test section and its contents. Here a rotating point source containing ^{57}Co rotates around the object to provide a flux of photons along each line of response. Before the activity is introduced, the pump is turned on and the system allowed to run for several minutes. Before the labeled fibers are added to the tank the flow rate is adjusted, and the camera set to acquire data. The radioactive fibers are then added to the tank and allowed to be pumped though the system. At this point data acquisition is begun. Each scan is allowed to run until 100,000,000 events are detected or 1 h has elapsed.

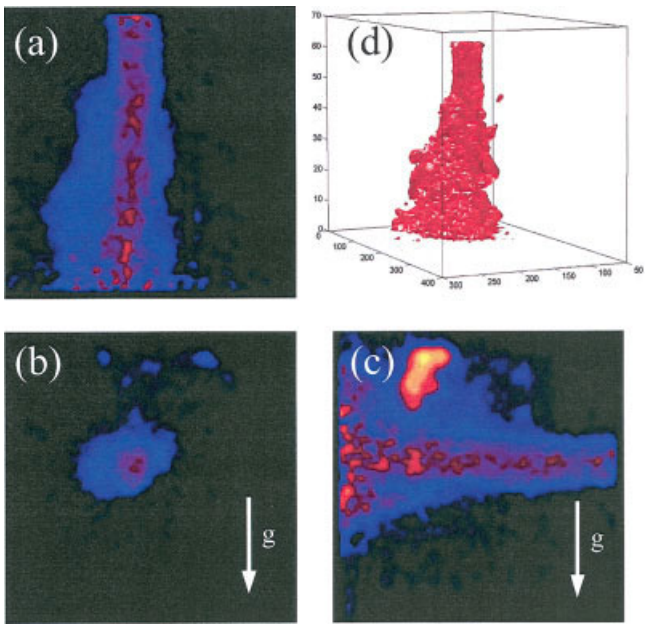

Figure 6. Four views of the activity profile for the case in which the tracer fibers were not well-mixed after the expansion.

We define this case as plug flow type behavior. The image was acquired using the R48 tracer fibers with the upstream velocity set at 0.5 *m/s* (see Table 1). Image (a) represents the top view, (b) is a cross-sectional view at $x/R_o = 1.00$, (c) is a side view, and (d) is a 3-D reconstruction of the activity distribution. No color map is included in (a) through (c). The blue color, however, represents a lower concentration than the red color. [Color figure can be viewed in the online issue, which is available at www.interscience.wiley.com.]

Results and Discussion

In this section, we discuss the qualitative behavior of this suspension as a function of velocity. As shown in Table 1, we recorded four cases in which the tracer fibers were well mixed after the expansion. We defined these cases as "fluidized," and the observed flow was qualitatively similar to that reported by Salmela & Kataja [2005]. The size of the recirculation zone is shown in Figure 3 for these cases only. It should be noted that the length of the recirculation zone L_R has been scaled to the height of the step h_s. It is difficult to compare our results quantitatively to either those reported by Salmela and Kataja (2005), as we have a different step size and suspension concentration, or to those for a corresponding Bingham fluid, as the rheological properties of the suspension are difficult to characterize properly.

We begin the discussion of the effect of velocity by examining Scan 2, see Table 1 and Figure 4. As with all cases presented three views are provided; a top view, a side view, and a cross-sectional view. The top and side views are slices from the centre of the test section in planes orthogonal to the viewing direction. As shown, these images are qualitatively similar to those reported by Moraczewski et al. (2005) in that we see a central jet surrounded by a recirculating zone. There are three observations that can be made immediately from this result. First, the fibers are not distributed evenly through the imaged-volume. An asymmetry is apparent in Figure 4c in which there is a higher-concentration of tracer fibers at the bottom of the tube when compared to the top. This feature was found in all fluidized cases examined and may result from gravitational effects, albeit via a complicated mechanism. Second, there is an annular region between the jet, and the recirculation zone with a concentration that is lower than the average concentration of the suspension. In other words, we observe a region with particle depletion. Finally, in the center of the recirculation zones the concentration of tracer particles is significantly larger than the average concentration. The last two observations have been reported by Moraczewski et al. (2005). We attempt to quantify these features by examining the radial concentration profiles at different axial positions, see Figure 5a and b. In these figures we have normalized the concentration to the bulk concentration of the suspension, that is, 0.4 wt%. Radial and axial distances have been normalized by the radius of the larger pipe; and the axial origin $x = 0$, is set at the step. We speculate that the concentration-depletion zone results from the water

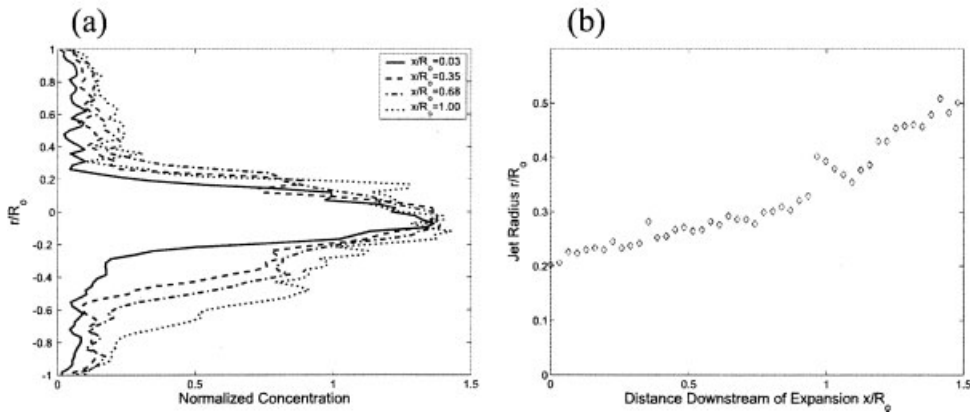

Figure 7. Two views of the activity profile for the case in which the tracer fibers were not well-mixed after the expansion.

We define this case as plug flow type behavior. The image was acquired using the R48 tracer fibers with the upstream velocity set at 0.5 *m/s* (see Table 1). Image (a) represents the concentration profile in the radial direction at four different axial positions. This data was acquired from Figure 6a. Image (b) represents the width of the activity profile as a function of axial position.

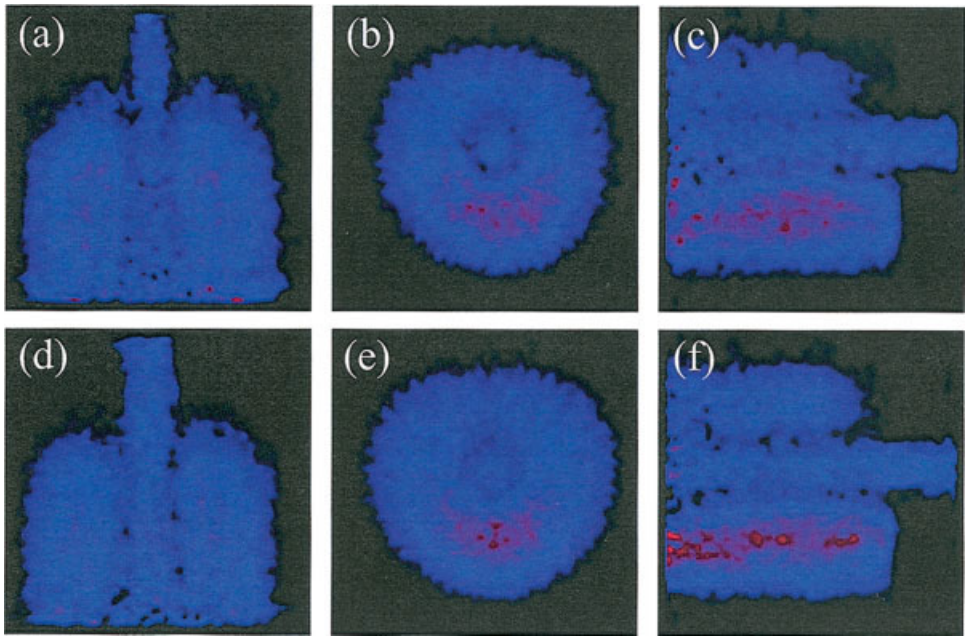

Figure 8. Two cases in which the tracer fibers were well-mixed after the expansion.

In images (a)–(c) we examine the case in which the upstream velocity was set at 0.9 *m/s* with the R100 tracer fibers. Images (d)–(f) represent the case with the R14 tracer fibers. The images in the first column ((a) and (d)) represent the top view. The images in the second column represent the cross-sectional view at $x/R_o = 0.57$. The remaining two images represent the side-view. [Color figure can be viewed in the online issue, which is available at www.interscience.wiley.com.]

layer formed in the upstream tube. It is commonly understood that a water layer forms on the periphery of a pipe with a flowing pulp fiber suspension. We have characterized both the radius of the jet and thickness of the concentration-depletion layer in Figure 5c as a function of axial position. As shown, we see that the radius of the jet remains essentially constant over the distance reported, while the size of the concentration-depletion layer decreases slightly. These were determined using an edge-detection algorithm. Finally, as shown in Figure 5d, the average concentration of the jet increases with axial position. In this case we see a 50% increase in the concentration in the central portion of the tube, and advance the argument that this results from the deceleration of the jet.

At this point we turn our attention to the second type of behavior observed, that is, plug flow. We observed this in one of the scans conducted, namely Scan 1, which was conducted at an upstream velocity of 0.5 m/s. As shown in Figure 6, the tracer fibers were not well distributed after the expansion plane, and travelled as a plug through the region visualized. Clearly, at this lower velocity, the shear imparted by the fluid is insufficient to disrupt the network. It must be noted that during imaging, the central jet may be slowly meandering or folding as it travels down the length of the tube. This feature can not be captured as the image acquired is averaged over a long time. We characterize these curves by showing the radial concentrations and the size of the central jet in Figure 7. As shown, we see that the tracer fibers spread radially with increasing axial distance. The mechanism by which these fibers spread is difficult, if not impossible, to ascertain from these figures alone, as the jet may me-

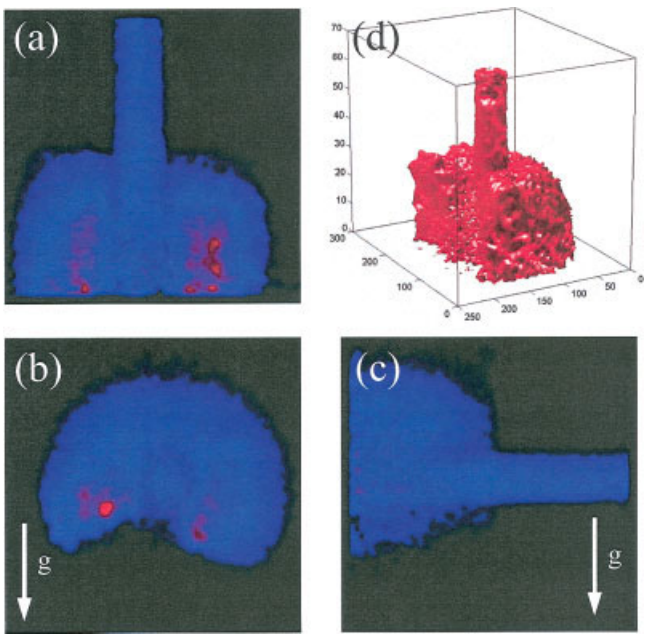

Figure 9. Four views of the activity profile for the case in which the tracer fibers were partially-mixed after the expansion.

The image was acquired using the R14 tracer fibers with the upstream velocity set at 0.5 *m/s* (see Table 1). Image (a) represents the top view, (b) is a cross-sectional view at $x/R_o = 0.57$, (c) is a side view, and (d) is a 3-D reconstruction of the activity distribution. [Color figure can be viewed in the online issue, which is available at www.interscience.wiley.com.]

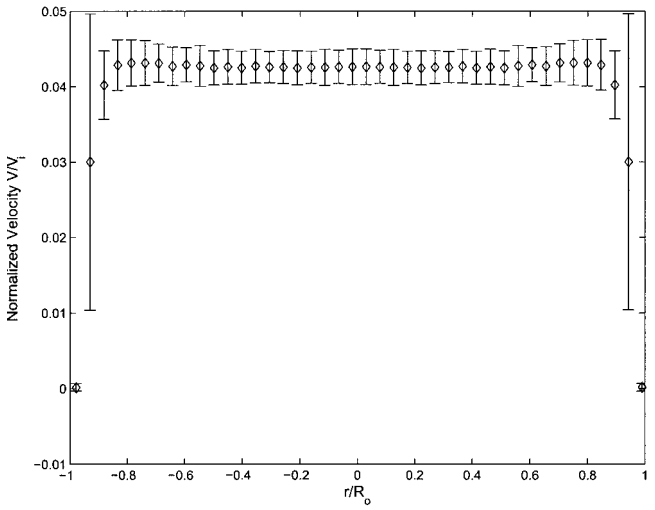

Figure 10. Velocity profile of the suspension as measured using UDV.

Six experiments were conducted in which the upstream velocity V_i set in the range from 0.5 to 1.0 *m/s*. The error bars represents the standard deviation determined from the average of this data set.

ander during the imaging period. In other words, we can not ascertain if the tracer fiber mixing results from shear induced migration or from the stability of the jet. One of the striking features in this image is the relatively large localized concentration of activity near the top of the tube in Figure 7c. We are uncertain of the origin of this, but its presence confirms the fact that mixing does not take place at this velocity.

At this point we compare the effect of particle size by examining two cases conducted at the same velocities using different length fractions. In the first comparison, we examine scans 5 and 6 in which we compare the distribution of the R100 and R14 tracer fibers at 0.9 m/s (see Figure 8). As shown, the distribution of these tracer fibers appear somewhat similar. In both cases the features reported in the previous section are apparent; that is an asymmetry in the vertical direction, a depletion layer between the central jet, and the recirculation zone, and particle accumulation in the lower recirculating zone. We find that no significant differences in the distributions are apparent between these two cases.

In the second comparison, we examine the distributions of the R48 and R14 fibers at 0.5 m/s as given as scans 1 and 4 in Table 1. The results for scan 1 have been shown earlier as Figure 6. Here it is apparent that the tracer fibers are not well-mixed after the expansion. With the R14 fibers, however, we find that the tracer fibers are well-mixed in the upper portion of the channel only (see Figure 9). In the upper portion of the channel we observe the depletion zone between the central jet and the outer portions of the channel. It should be noted that during this trial it was visually observed that the lower portion of the channel was static. We do not interpret these results as quantitative evidence that their is a difference between the motion of these two classes of fibers. We speculate that this result occurred due to the fact that the experimental protocol was not the same as the other scans. The pulp in the test section was allowed to settle

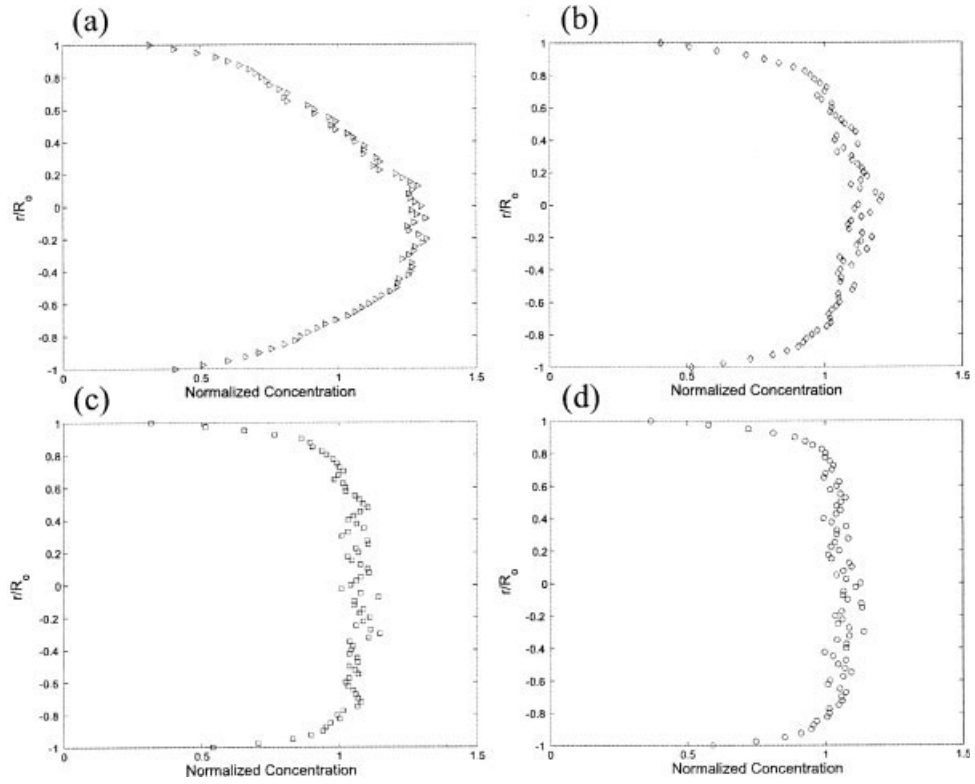

Figure 11. Concentration profile downstream of the expansion.

(a) Scan 1, (b) Scan 2, (c) Scan 5 and (d) Scan 6. Details of each experiment are given in Table 1.

over several days prior to the scan and was not mixed prior to the start of the scan. Furthermore, when the scan was conducted the flow rate began high and was lowered, as opposed to being ramped up to the targeted flow rate as in the subsequent scans. This resulted in the region with less fiber being fluidized first, and when the flow rate was dropped the region remained in motion. We have included this result as it is interesting to report the possibility of a stable, static region in this type of device.

Far downstream of the expansion ($x/R_o = 20$) we were able to measure both the concentration distribution using PET and the velocity profile using ultrasound Doppler velocimetry (UDV), a commercial device obtained from Signal Processing SA. For all flow rates tested, the velocity profiles at this point were similar and displayed plug like behavior. As shown in Figure 10, a velocity boundary layer exists near the walls of the pipe in the region $r/R_o > 0.8$. We display the concentration profiles at this point for four different cases (see Figure 11). What is apparent from these figures is that the concentration profile is not necessarily similar to the velocity profile. We speculate that the tracer fibers, trapped in small flocs at the inlet, are not sufficiently disrupted by the shear at the step to redistribute themselves evenly downstream. As the flow rate is increased more mixing is induced and a more even radial distribution is evident.

Summary and Conclusion

Positron emission tomography (PET) was used to investigate the dynamics of a 0.4% (wt) fiber suspension flowing through an axisymmetric 1:5 sudden expansion. Six scans were conducted in which both the upstream velocity, and the size of tracer particles labelled were varied. Images were taken upstream and downstream of the expansion plane with the upstream velocity being varied from 0.5 to 0.9 m/s. The expansion plane imparts shear that disrupt the fiber network causing measurable changes in the local fiber concentration. Two distinct regions were clearly distinguished: plug-like, in which the tracer fibers were not mixed through the entire volume of the expansion, and fluidized, in which the tracer fibers were well mixed. Our results for the fluidized case are worth highlighting as we found that concentration inhomogeneities exist. We consider these to be the most significant findings in this work, and are currently trying to develop a mechanistic understanding of these phenomena.

Acknowledgments

Financial support from the Natural Sciences and Engineering Research Council of Canada and the TRIUMF Life Sciences program are gratefully acknowledged.

Literature Cited

Altobelli SA, Fukushima E, Mondy LA. "Nuclear Magnetic Resonance imaging of Particle Migration in Suspensions Undergoing Extrusion". *J. Rheol.* 1997;41(5):1105–1115.

Autobelli SA, Givler RC, Fukushima E. "Velocity and concentration measurements of suspensions by nuclear magnetic resonance imaging". *J. Rheol.* 1997;35(5):721–734.

Arola D, Powell R, McCarthy M, li T-Q, Ödberg L. "NMR Imaging of Pulp Suspension Flowing through an Abrupt Pipe Expansion". *AIChE J.* 1998;44(12):2597–2606.

Duffy GG. Titchener AL. "The Disruptive Shear Stress of Pulp Networks". *Svensk. Papperstidn.* 1975;13:474–479.

Hammad KJ, Ötügen MV, Vradis G, Arik E. "Laminar Flow of a Nonlinear Viscoplastic Fluid Through an Axisymmetric Sudden Expansion". *ASME J.* 1999;121:488–495.

Jossic L, Briguet A, Magnin A. "Segregation Under flow of Objects Suspended in a Yield Stress Fluid and NMR Imaging Visualization". *Chem. Eng. Sci.* 2002;57:409–418.

Karino T, Goldsmith HL. "Flow Behavior of Blood-Cells and Rigid Spheres in an Annular Vortex". *Phil., Trans. R. Soc. London, Ser. B.* 1977;279:413–445.

Kerekes RJ, Soszysnki RM, Tam Doo PM. "The flocculation of pulp fibres". *Fund. Res. Symp., Oxford* 1985;1:265–310.

Knoess C, Sibgel S, Smith A, Newport D, Richerzhagen N, Winkler A, Jacobs A, Goble R-N, Graf R, Wienhard K, Heiss W-D. "Performance Evaluation of the microPET R4 PET Scanner for Rodents". *Eur. J. Nucl. Mol. Imaging.* 2003;30(5):737–747.

Latornell DJ, Pollard A. "Some Observations on the Evolution of Shear Layer Instabilities in Laminar Flow Through Axisymmetric Sudden Expansions", *Phys. Fluids.* 1986;29:2828–2835.

Leighton D, Acrivos A. "The Shear-Induced Migration of Particles in Concentrated Suspensions". *J. Fluid Mech.* 1987;181:415–439.

Magagno EO, Hung TK. "Computational and Experimental Study of a Captive Annular Eddy", *J. Fluid Mech.* 1967;28:43–64.

Mok S-P, Wang C-H, Chen J-C, Liu R-S. "Performance Evaluation of the High Resolution Small Animal PET Scanner". *Biomed. Eng. Appl Basis Comm.* 2003;15(4):143–149.

Moraczewski T, Tang H, Shapley N. "Flow of a Concentrated Suspension Through an Abrupt Axisymmetric Expansion Measured by Nuclear Magnetic Resonance Imaging". *J. Rheol.* 2005;49(6):1409–1428.

Phillips RJ, Armstrong RC, Brown RA, Graham AL, Abbott JR. "A Constitutive Equation for concentrated suspensions that accounts for shear-induced particle migration". *Phys. Fluids* 1992;4:30–40.

Salmela J, Kataja M. "Floc Rupture and Re-Flocculation in Turbulent Shear Flow". *Fund. Res. Symp., Cambridge* 2005;1:35–50.

Sossi V, Camborde M-L, Tropini G, Newport D, Rahmim A, Ruth T-J. "The Influence of Measurement Uncertainties on the Evaluation of the Distribution Volume Ration and Binding potential in Rat Studies on a microPET R4: a Phantom *Stud. Phys. med. Biol.* 2005;50(12):2859–2869.

Thalen N, Wahren D. "An Experimental Investigation of the Shear Modulus of Model Fibre Networks". *Svensk. Papperstidn.* 1964;67(11): 474–480.

Thalen N, Wahren D. "Shear Modulus and Ultimate Shear Strength of Some Pulp Fibre Networks", *Svensk. Papperstidn.* 1964;67(7):259–264.

Manuscript received July 19, 2006, and revision received Nov. 22, 2006.